Molecular and crystal structure of the clathrochelate complex $FeDm_3(BF)_2 \cdot C_6H_6$ and parameters of its ^{57}Fe Mössbauer spectra

I. I. Vorontsov,[a]★ K. A. Lysenko,[a] K. A. Potekhin,[a] M. Yu. Antipin,[a] Ya. Z. Voloshin,[b] E. V. Pol'shin,[c] and O. A. Varzatskii[b]

[a]*A. N. Nesmeyanov Institute of Organoelement Compounds, Russian Academy of Sciences, 28 ul. Vavilova, 117813 Moscow, Russian Federation. Fax: +7 (095) 135 5085. E-mail: ivorontsov@xray.ineos.ac.ru*

[b]*State Research Center of the Russian Federation "L. Ya. Karpov Institute of Physical Chemistry," 10 ul. Vorontsovo Pole, 103064 Moscow, Russian Federation. Fax: +7 (095) 975 2450. E-mail: voloshin@cc.nifhi.ac.ru*

[c]*Institute of Geochemistry, Mineralogy, and Ore Formation, National Academy of Sciences of Ukraine, 34 ul. Palladina, 252149 Kiev, Ukraine*

The molecular and crystal structure of the macrobicyclic complex $FeDm_3(BF)_2 \cdot C_6H_6$ was established by X-ray diffraction analysis at 138, 208, and 291 K. The X-ray diffraction data were compared with the ^{57}Fe Mössbauer spectral parameters of this complex in the temperature range of 135—290 K. A substantial disagreement between the experimental values of quadrupole splitting and the corresponding values calculated based on the concept of partial quadrupole splitting was attributed to the displacement of the Fe atom from the center of the cavity of the macrobicyclic ligand and to the distortion of the axial symmetry of the electron density distribution about the metal atom.

Key words: clathrochelate complexes, iron(II), ^{57}Fe Mössbauer spectra, X-ray diffraction study, molecular structure, temperature dependences, electron density distribution.

Structural phase transitions in crystals of clathrochelate complexes[1] containing the low-spin iron(II) ion in the three-dimensional cavity of the macrobicyclic ligand can be efficiently studied with the use of X-ray diffraction analysis in combination with ^{57}Fe Mössbauer spectroscopy. Thus, both structural phase transitions (at 190(3) and 290(3) K) in the crystal of cyclohexadione-1,2-dioximate (nioximate) hexadecylboronate complex $FeNx_3(BHd)_2$, which have been found by X-ray diffraction analysis,[2] are also manifested in the ^{57}Fe Mössbauer spectra. The quadrupole splitting (QS) determined by the gradient of the electric field at the nucleus of the central atom changes stepwise in the vicinity of the phase-transition points. The relation between the QS value and the geometry of the coordination environment about the Fe atom was used for the prediction of structures of low-spin iron(II) complexes.[3—6] In particular, the relation between QS at the Fe nucleus and the geometry of its distorted trigonal-prismatic coordination polyhedron formed by six N atoms was established within the framework of the model of partial QS (PQS)[7] (Fig. 1). In this case, the following assumptions were used[8]: (1) the trigonal-prismatic environment about the Fe^{II} ion has the axial symmetry C_3; (2) QS in ^{57}Fe Mössbauer spectra can be represented by the sum of PQS of the individual ligands that form the coordination polyhedron about the central Fe^{II} ion (the equivalence of the donor groups of the ligand was postulated); (3) PQS was taken to be constant for the particular ligand at the given electronic configuration.

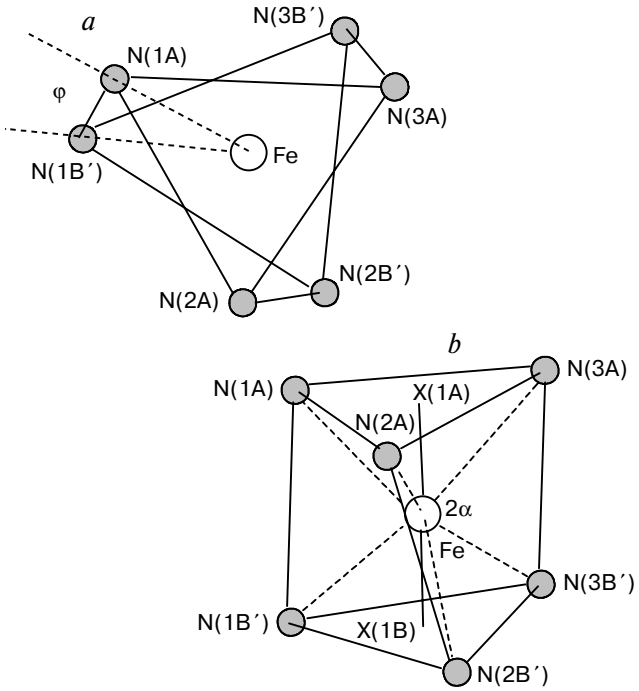

Fig. 1. Distorted trigonal-prismatic coordination environment about the Fe^{II} ion formed by six N atoms: the projection along the threefold axis (*a*) and the side view (*b*). The angles of rotation (distortion) φ, which characterize deviation from the ideal trigonal prism, about the threefold axis and the chelate angle 2α are shown; X(1A) and X(1B) are the centers of the bases of the coordination polyhedron.

Published in Russian in *Izvestiya Akademii Nauk. Seriya Khimicheskaya,* No. 12, pp. 2053—2061, December, 2000.

1066-5285/00/4912-2018 $25.00

The geometry of this type of complexes is characterized by the distortion angle φ, which changes from the trigonal prism (TP, φ = 0°) to the trigonal antiprism (TAP, φ = 60°), and the bite angle α (half-angle in the chelate ring) (see Fig. 1). The dependence of QS on the geometric parameters of the coordination polyhedron can be represented[8] as QS = $f \cdot$ PQS, where $f = 12 - 18\cos^2\alpha/\cos^2(\varphi/2)$.[7] The α angle is virtually constant in this series of compounds (38.6—39.5°). Therefore, QS depends primarily on the distortion angle φ. For uncharged macrobicyclic iron(II) dioximates, the best agreement between the experimental and calculated QS values was observed[8] at PQS = 0.5 mm s^{-1}.

The temperature dependences of QS for the complex $FeDm_3(BF)_2$ (**1**) reported previously[6] suggest the occurrence of the structural phase transition in the crystals of **1** at 200 K. In the present work, a single crystal of $FeDm_3(BF)_2 \cdot C_6H_6$ was studied by X-ray diffraction analysis at 138, 208, and 291 K and by ^{57}Fe Mössbauer spectroscopy in the temperature range of 135—290 K.

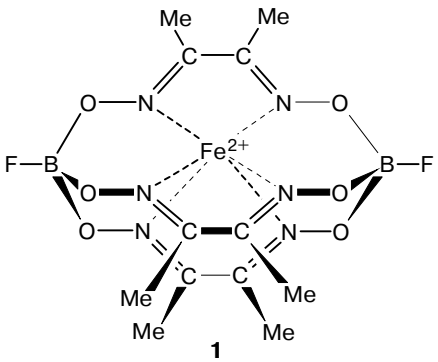

1

Experimental

Complex **1** was prepared according to a procedure reported previously.[9]

Synthesis of the clathrochelate $^{57}FeDm_3(BF)_2$. A mixture of metallic iron containing the ^{57}Fe isotope (30 mg, 0.54 mmol), nioxime (300 mg, 2.1 mmol), and an excess of $BF_3 \cdot O(C_5H_5)_2$ (1 mL) in Bu^nOH (10 mL) was refluxed for 30 h until the metal was completely dissolved and liberation of H_2 ceased. Two portions of nioxime (142 mg, 1 mmol) and $BF_3 \cdot O(C_5H_5)_2$ (0.5 mL) were added in the course of the reaction. The orange-yellow precipitate that formed was filtered off and washed with ethanol, diethyl ether, and hexane. Then the precipitate was recrystallized from hot chloroform followed by precipitation with hexane. The yield was 210 mg (87%).

Single crystals of $FeDm_3(BF)_2 \cdot C_6H_6$ and $^{57}FeDm_3(BF)_2 \cdot C_6H_6$ were prepared by slow evaporation of their saturated solutions in benzene at room temperature over several weeks.

X-ray diffraction study. The crystal structure of complex **1** was studied at 138, 208, and 291 K on an automated Syntex $P2_1$ and Bruker SMART diffractometers (λ(Mo-Kα) = 0.71073 Å). The X-ray data sets were collected from isometric crystals. The intensities of all measured reflections were corrected for the Lorentz and polarization factors.[10] Absorption was ignored. The principal crystal-structural data are given in Table 1.

The structure of $FeDm_3(BF)_2 \cdot C_6H_6$ was solved by the direct method and refined based on F^2 by the full-matrix least-squares method with anisotropic thermal parameters for nonhydrogen atoms using the SHELXTL-PLUS program package.[11] The completely resolved disordered positions of the N and O atoms were revealed from the difference Fourier synthesis. We failed to resolve possible disordered positions of the C atoms due to their proximity. The positions of the H atoms at 208 and 291 K were calculated geometrically and included in the refinement using the riding model with fixed isotropic displacement parameters, which were equal to $1.2U_{eq}$ for the

Table 1. Principal crystal-structural data for complex **1** and the results of the refinement at 138, 208, and 291 K

Parameter	138 K	208 K	291 K
Crystal habitus	Prism	Prism	Prism
Crystal dimensions/mm	0.20×0.30×0.60	0.20×0.30×0.60	0.20×0.30×0.70
Diffractometer	Syntex $P2_1$	Syntex $P2_1$	Bruker SMART
Radiation	Mo-Kα	Mo-Kα	Mo-Kα
a/Å	14.227(4)	14.225(9)	14.3585(6)
b/Å	13.441(3)	13.487(8)	13.5787(6)
c/Å	11.712(3)	11.776(8)	11.8435(5)
V/Å^3	2239.6(10)	2259(3)	2309.1(2)
Space group	*Pnma*	*Pnma*	*Pnma*
Z	4	4	4
d_{calc}/g cm^{-3}	1.589	1.576	1.542
μ/mm^{-1}	0.740	0.733	0.717
Scanning technique	θ/2θ	ω/2θ	ω
$2\theta_{max}$/deg	82	60	63
Number of independent reflections	8572	3402	3849
Number of reflections with $F^2 > 2\sigma(F^2)$	4891	2201	2578
$R_1(F)$	0.060	0.049	0.045
$wR_2(F^2)$	0.129	0.121	0.109
GOOF	1.072	0.862	1.012

benzene molecule and $1.5U_{eq}$ for the Me groups, where U_{eq} are equivalent isotropic displacement parameters of the corresponding atoms. At 138 K, the positions of the H atoms were revealed from the difference Fourier synthesis and refined isotropically. The final reliability factors are given in Table 1. The coordinates of atoms are deposited in the Cambridge Structural Database.

^{57}Fe Mössbauer spectroscopy. The ^{57}Fe Mössbauer spectra of single crystals of $^{57}FeDm_3(BF)_2 \cdot C_6H_6$ were measured on an YaGRS-4M spectrometer equipped with a cryostat. Sample was placed into a plastic cell and kept fixed. Measurements were carried out using a vibrator operating in the constant acceleration mode with accumulation in 256 channels of the analyzer. The ^{57}Co isotope in the chromium matrix was used as the source of γ radiation. The spectrometer was calibrated against α-Fe_2O_3. The isomeric shifts were measured relative to sodium nitroprusside with an accuracy of 0.01 mm s^{-1}. The accuracy of determination of QS was ±0.005 mm s^{-1}. The minimum width of absorption lines in the spectrum of the standard sample of sodium nitroprusside was 0.24 mm s^{-1}.

Results and Discussion

Crystal structure. Investigation of the temperature dependence of the unit cell parameters of the crystal of complex **1** in the range of 138—291 K with a step of ~10 K did not reveal anomalies of thermal expansion of the crystal, which could be indicative of structural changes. The parameters and volume of the unit cell are adequately approximated by linear temperature dependences. In the temperature range under examination, the translational symmetry of the crystal and the space group remained unchanged (see Table 1). No changes in the molecular packing, which could be associated with the phase transition, were found.

The molecules of complex **1** are packed in stacks parallel to the crystallographic direction [100]. In the projection onto the *bc* plane, the molecular stacks are arranged in a herringbone fashion. There are no shortened intermolecular distances in the crystal. The benzene molecules of solvation occupy special positions (the C(1S) and C(4S) atoms lie on a mirror plane) and are located in channel between the stacks. Apparently, interactions between the molecules of complex **1** and the benzene molecules are rather weak because the benzene molecules of solvation were eliminated upon storage in air for one month.

The conventional refinement of the structure converged to rather high R_1 factors (0.116 and 0.072 at 138 and 291 K, respectively) and led to substantial shortening of the B—O (by 0.049 and 0.037 Å at 138 and 291 K, respectively) and N=C (by 0.033 and 0.027 Å at 138 and 291 K, respectively) bond lengths compared to the values typical of this type of complexes (1.48 and 1.32 Å for B—O and N=C, respectively). In addition, the anisotropic displacement parameters for the O and N atoms in the tangential direction with respect to the threefold pseudoaxis of the molecule passing through the B atoms have anomalously high values (Fig. 2). Moreover, these parameters remain virtually unchanged as the temperature changes (on the average, 0.289 and 0.298 Å^2 for the O atoms and 0.148 and 0.153 Å^2 for the N atoms at 138 and 291 K, respectively). Generally, such a behavior is determined by the unresolved statistical disorder of atoms over two positions.[12]

Actually, two equally probable positions for the O and N atoms each were revealed from the difference Fourier synthesis (the occupancies of these positions were refined at all temperatures) after which the R_1 factors were virtually halved (0.060 and 0.045 at 138 and 291 K, respectively). At the same time, the anisotropic displacement parameters (see Fig. 2) and the B—O and N—O distances acquired reasonable values (Table 2). We failed to reveal the disorder of the C atoms due to the proximity of their possible positions. No evidence of disorder was found for the Fe atom, which occupies a special position on the mirror plane *m* located perpendicular to the molecular threefold pseudoaxis.

The disorder in the crystal may result from superposition of two conformers, which are either related by the mirror plane or twisted about the threefold axis. In the

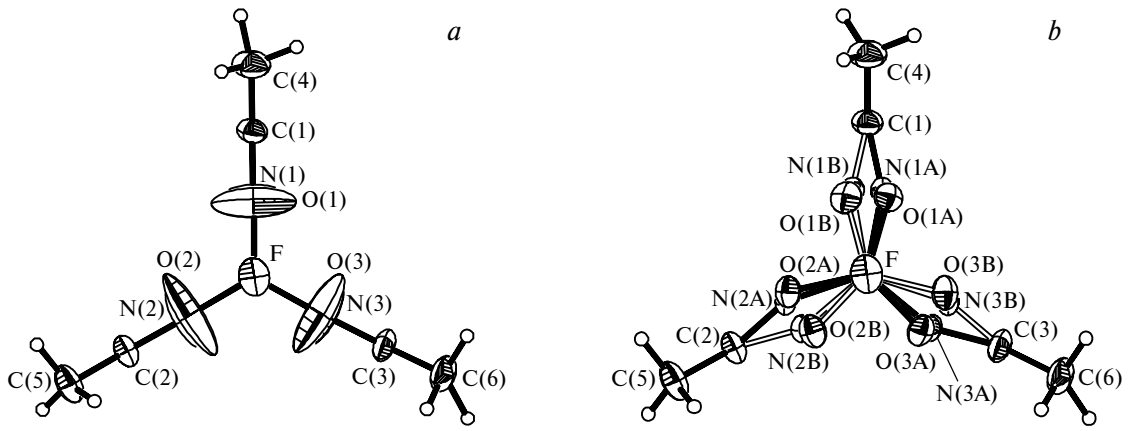

Fig. 2. Projection of the complex along the threefold pseudoaxis of molecule **1** at 138 K; the F atom screens the B and Fe atoms: *a*, the results of the conventional refinement; *b*, the refinement after resolution of the disorder. The atoms are represented by 50%-probability ellipsoids of anisotropic displacements.

Table 2. Selected bond lengths (d) in complex **1** at 138, 208, and 291 K

Bond	d/Å		
	138 K	208 K	291 K
Fe—N(1A)	1.930(2)	1.931(3)	1.926(5)
Fe—N(2A)	1.928(2)	1.916(4)	1.919(5)
Fe—N(3A)	1.935(2)	1.921(4)	1.932(4)
N(1A)—C(1)	1.328(3)	1.325(5)	1.325(5)
N(2A)—C(2)	1.330(3)	1.312(5)	1.311(5)
N(3A)—C(3)	1.361(3)	1.355(5)	1.339(5)
O(1A)—N(1A)	1.381(3)	1.378(5)	1.387(5)
O(2A)—N(2A)	1.371(3)	1.379(5)	1.381(5)
O(3A)—N(3A)	1.364(3)	1.371(5)	1.378(5)
B—O(1A)	1.477(3)	1.479(4)	1.469(4)
B—O(2A)	1.501(2)	1.482(4)	1.495(3)
B—O(3A)	1.455(3)	1.433(4)	1.452(4)
Fe—N(1B)	1.891(2)	1.899(3)	1.900(5)
Fe—N(2B)	1.890(2)	1.890(4)	1.901(5)
Fe—N(3B)	1.893(2)	1.895(4)	1.893(5)
N(1B)—C(1)	1.319(3)	1.316(5)	1.311(5)
N(2B)—C(2)	1.336(3)	1.322(5)	1.318(5)
N(3B)—C(3)	1.293(3)	1.278(5)	1.286(5)
O(1B)—N(1B)	1.371(3)	1.355(5)	1.371(5)
O(2B)—N(2B)	1.377(3)	1.381(5)	1.375(5)
O(3B)—N(3B)	1.376(3)	1.381(5)	1.377(5)
B—O(1B)	1.485(3)	1.499(4)	1.490(4)
B—O(2B)	1.483(3)	1.466(4)	1.461(3)
B—O(3B)	1.519(2)	1.501(4)	1.513(3)
C(1)—C(4)	1.487(2)	1.487(3)	1.486(3)
C(2)—C(5)	1.491(2)	1.494(3)	1.501(2)
C(3)—C(6)	1.492(2)	1.486(3)	1.497(3)
F—B	1.364(2)	1.369(3)	1.364(2)
C(1S)—C(2S)	1.377(3)	1.374(4)	1.371(3)
C(2S)—C(3S)	1.388(3)	1.352(4)	1.359(4)
C(3S)—C(4S)	1.381(2)	1.371(4)	1.360(4)
C(1)—C(1)*	1.437(3)	1.430(4)	1.431(4)

* The symmetry operation: x, $-y + 1/2$, z.

first case, possible positions of the C atoms should be far removed from each other due to almost planar structures of the dimethylglyoximate fragments, which is in contradiction with the real situation. Apparently, complex **1** in the crystal is disordered over two positions, which differ in the direction of twisting (either clockwise or counterclockwise) about the threefold pseudoaxis of the molecule. As a result, the statistical plane m occurs in the crystal due to the superposition of two mirror-related conformers. The overall view of one of the equally probable conformers of complex **1** and the atomic numbering scheme are shown in Fig. 3.

To exclude the appearance of disorder due to the symmetry restrictions caused by the mirror plane m, we carried out the additional refinement of the structure in the noncentrosymmetric space group $Pna2_1$ at 138 K. In this case, an analogous equally probable disorder of the complex over two positions was revealed from the difference Fourier synthesis, which supported the conclusion about the statistical occurrence of the plane m in the crystal. The two disordered positions are related by the

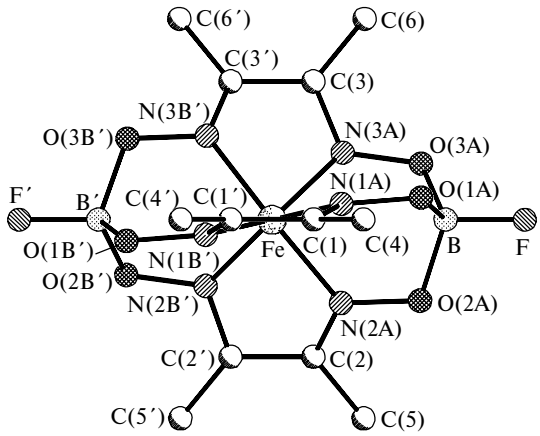

Fig. 3. Overall view and the atomic numbering scheme for complex **1**. The hydrogen atoms of the Me groups are omitted. The atoms generated by the symmetry plane m passing through the Fe atom perpendicular to the threefold pseudoaxis are primed. The second conformer is generated by the mirror plane m.

mirror plane with an accuracy of 0.07 Å (the mean deviation of the positions of the nonhydrogen atoms). In the space group $Pna2_1$, the structure was refined to the R_1 factor of 0.076. In the course of refinement, substantial correlations between the coordinates of virtually all pairs of nonhydrogen atoms, which are related by the plane m in the space group $Pnma$, were found. The characteristic features of the molecular geometry discussed below take place in both space groups. However, the error of the determination of the bond lengths in the noncentrosymmetric space group $Pna2_1$ is almost four

Table 3. Principal bond angles (ω) in complex **1** at 138, 208, and 291 K

Angle	ω/deg		
	138 K	208 K	291 K
C(1)—N(1A)—O(1A)	117.2(2)	117.5(3)	117.4(4)
C(1)—N(1A)—Fe	116.8(2)	116.9(3)	117.2(3)
F—B—O(1A)	106.9(2)	106.3(2)	106.6(2)
O(1A)—B—O(2A)	110.7(2)	110.7(2)	110.7(2)
N(1A)—O(1A)—B	110.4(2)	110.4(3)	110.8(3)
N(1A)—C(1)—C(1)*	111.1(2)	111.2(2)	111.1(2)
N(1A)—C(1)—C(4)	122.5(2)	122.6(2)	122.6(3)
C(1)—N(1B)—O(1B)	115.1(2)	115.7(3)	115.7(4)
C(1)—N(1B)—Fe	119.9(2)	119.6(3)	119.7(3)
F—B—O(1B)	109.2(2)	108.6(2)	108.8(2)
O(1B)—B—O(2B)	111.2(2)	111.4(2)	111.1(2)
N(1B)—O(1B)—B	112.9(2)	112.5(3)	113.1(3)
N(1B)—C(1)—C(1)*	109.0(2)	109.4(2)	109.1(2)
N(1B)—C(1)—C(4)	124.6(2)	124.6(2)	124.3(3)
C(1)*—C(1)—C(4)	125.2(2)	124.9(2)	125.2(2)
C(2S)*—C(1S)—C(2S)	120.4(2)	118.9(4)	119.1(4)
C(1S)—C(2S)—C(3S)	119.8(2)	120.7(3)	120.1(3)
C(3S)*—C(4S)—C(3S)	119.6(2)	120.0(3)	120.7(3)
C(4S)—C(3S)—C(2S)	120.2(2)	119.8(4)	119.4(4)

* The symmetry operation: x, $-y + 1/2$, z.

times as large as that in the space group *Pnma*. Hence, hereinafter we will discuss the structure refined within the space group *Pnma*.

The molecular geometry of the clathrochelate (see Fig. 3) does not substantially change in the temperature range under study. The principal bond lengths and bond angles at 138, 208, and 291 K are given in Tables 2 and 3, respectively. Complex **1** has the molecular symmetry C_3 (the threefold pseudoaxis passing through the B and Fe atoms), which is close to D_3. The latter axis is not exact due to the difference in the distances from the Fe atom to the bases of the trigonal prism formed by the N atoms (at 138 K, 1.202(2) and 1.138(2) Å to the N(1A)—N(2A)—N(3A) and N(1B′)—N(2B′)—N(3B′) planes, respectively; see Fig. 1). The base sides of the prism are equal to within the experimental error. The same is true for the generatrices of the prism, which are 2.618(3) and 2.405(3) Å at 138 K and 2.623(5) and 2.394(5) Å at 291 K. The coordination polyhedron is intermediate between the trigonal prism and trigonal antiprism; the distortion angle φ is equal to 21.2°. The bases of the prism are parallel to one another (the angle between the normals to these bases is no larger than 1.4(3)° at all temperatures under study). The angle formed by the Fe atom with the centers of the prism, *viz.*, with X(1A) и X(1B), is close to 180° (see Fig. 1). This signifies that the Fe atom is displaced from the center of the coordination polyhedron formed by six N atoms by 0.034(4) Å (at 138 K) along the threefold pseudoaxis (this displacement is 0.026(6) and 0.023(6) Å at 208 and 291 K, respectively). Therein lies the substantial difference between complex **1** and clathrochelates containing identical α-dioximate fragments and linking groups, which have been studied previously (the so-called axial-meridian-symmetrical macrobicycles) and in which these displacements were not observed.[5]

For complex **1**, the experimental QS value (~0.7 mm s^{-1}) is twice as large as the value calculated within the framework of the PQS model (0.38 mm s^{-1}). In this case, one of the major concepts of the model regarding the equivalence of the PQS values for donor atoms is most probably inapplicable due to the fact that PQS depends substantially on the Fe—N distance. Thus, the displacement of the Fe ion from the center of the coordination polyhedron along the threefold axis found in this study leads to a significant increase in the gradient of the electric field at the nucleus and, as a consequence, to an increase in QS.

It should be noted that the experimental QS value for the desolvated complex $FeDm_3(BF)_2$ (0.90 mm s^{-1} at 298 K[8] and 1.05 mm s^{-1} at 77 K[9]) differs substantially (by ~0.2 mm s^{-1}) from that found in its benzene solvate **1** due, apparently, to a substantial effect of ordering in the crystals of the latter compound.

Therefore, X-ray diffraction study of the structure of complex **1** in the temperature range of 138—291 K did not reveal characteristic features indicative of structural phase transitions in the crystal. Apparently, broadening of the QS lines in the region of 200 K [6] is associated with elimination of the benzene molecules from the crystals of **1** in the course of Mössbauer spectral study resulting in the superposition of the QS spectra from regions characterized by different degrees of desolvation. In the present work, efforts were taken to prevent desolvation. Thus, the Mössbauer spectra were measured from crystals, which were kept in a saturated benzene vapor. In the temperature range of 135—290 K, the major parameters of the Mössbauer spectra (the quadrupole splitting and the isomeric shift (IS) determined by the s-electron density at the Fe nucleus) changed gradually without jumps as the temperature changes (Fig. 4).

Analysis of thermal motion. The coexistence of two equally probable mirror-related conformers in the crystal corresponds to the presence of two minima of the potential energy. In this case, transition from one minimum to another occurs through twisting of the molecule about the threefold pseudoaxis. The possibility of this conformational transition depends on the height of the barrier between two potential minima. Based on the value of this barrier, the disorder in the crystal of **1** can be described as either statistical or dynamic.

With the aim of determining the nature of disorder, we analyzed the anisotropic displacement parameters for the BO_3 fragments using Schomaker—Trueblood's rigid-body model.[13] We were interested in the libration amplitudes about the threefold pseudoaxis of the molecule. The B, F, and Fe atoms were also included in calculations of the corresponding tensors. These atoms are located on the molecular threefold pseudoaxis and should have no noticeable effect on the values of interest. The choice of the fragment was governed by the highest accuracy of determination of the coordinates and anisotropic displacement parameters of the O atoms (the quasi-high-angle refinement with the use of Dunitz—Seiler'

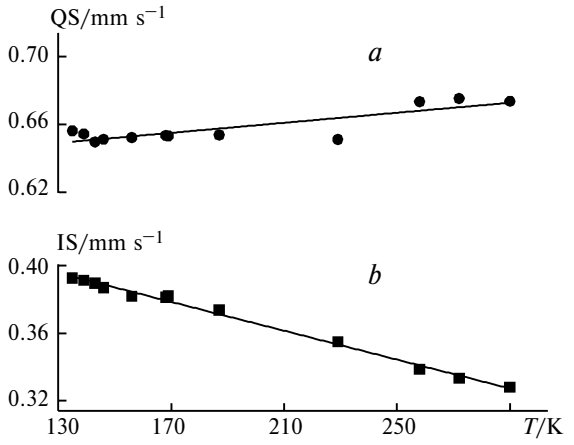

Fig. 4. Temperature dependences of the parameters of the ^{57}Fe Mössbauer spectra for complex **1**: *a*, quadrupole splitting (QS); and *b*, isomeric shift (IS). The vertical sizes of the symbols characterize the mean error of the determination of the corresponding values (0.005 mm s^{-1}).

Table 4. Analysis of thermal librations of the BO_3 fragments about the threefold axis in complex **1**

Parameter	138 K	208 K	291 K
Eigenvalue of the libration tensor L_1/deg^2	11(2), 16(2)	14(3), 15(3)	24(3), 31(4)
Eigenvector corresponding to L_1	0.42, 0.90, 0.10; 0.21, 0.97, 0.15	0.50, −0.86, 0.15; 0.15, −0.97, 0.24	0.18, −0.96, 0.22; 0.05, −0.99, −0.03
R_u Factor	0.022, 0.021	0.024, 0.020	0.015, 0.017
$<\Delta U^2_{ij}>^{1/2}$	0.0003, 0.0003	0.0005, 0.0006	0.0004, 0.0005
$<\sigma^2(U_{ij})>^{1/2}$	0.0006, 0.0006	0.0015, 0.0016	0.0011, 0.0011

Note. The orthonormal axes of coordinates *0X*, *0Y*, and *0Z* are codirected with the principal translations of the crystal lattice; $<\Delta U^2_{ij}>^{1/2}$ is the mean discrepancy between the experimental and calculated anisotropic displacement parameters; $<\sigma^2(U_{ij})>^{1/2}$ is the mean error of the determination of the experimental values U_{ij}.

weighting scheme[14] was used in the least-squares procedure). All calculations were carried out using the THMA-11 program package.[15] The principal results of analysis are given in Table 4. At all temperatures, the R_u factor (characterizing the discrepancy between the calculated and experimental U_{ij} values) was ~2%, which made it possible to consider the fragments under examination as rigid bodies.

The maximum mean amplitudes of librations L_1 correspond to librations about the molecular threefold pseudoaxis. The L_1 values for two independent BO_3 groups are virtually identical at all temperatures under study and are, on the average, 14(2) and 25(5) deg^2 at 138 and 291 K, respectively.

The angle between two possible orientations of the BO_3 group (hereinafter denoted as $2\theta_0$) is independent of the temperature and is equal to ~32°. In the harmonic approximation, the probability density function $P(\theta)$ (θ is the angle of rotation of the BO_3 group about the threefold axis) for the libration about two possible equilibrium positions specified by the angle $\pm\theta_0$ can be represented as the normalized sum of two Gaussian functions:[16]

$$P(\theta) = 0.5(2\pi L_1)^{-1/2}|\exp[-(\theta - \theta_0)^2/2L_1] + \exp[-(\theta + \theta_0)^2/2L_1]|.$$

The $P(\theta)$ plot for the librations of the BO_3 groups at 138 and 298 K is shown in Fig. 5 from which it can be seen that at $\theta = 0°$ the probability density $P(\theta)$ corresponding to the conformational transition through the potential barrier between two equilibrium positions is very small even at room temperature.

Then, the potential-energy curve $V(\theta)$ can be constructed and the potential barrier between two energy minima can be estimated with the use of the Boltzmann probability density formula $P(\theta) = A\exp|-V(\theta)/(RT)|$ (the constant A is calculated on the assumption that $V = 0$ at $\theta = \theta_0$, R is the universal gas constant, and T is the temperature). The potential-energy curve constructed based on the X-ray diffraction data at 138 K is shown in Fig. 5, where the values $0.5RT$ at 138 and 298 K are also given.

It is interesting to compare the disorder revealed in complex **1** with that observed in *para*-terphenyl.[16] Due to the presence of the phase transition (the temperature of the phase transition or the critical temperature

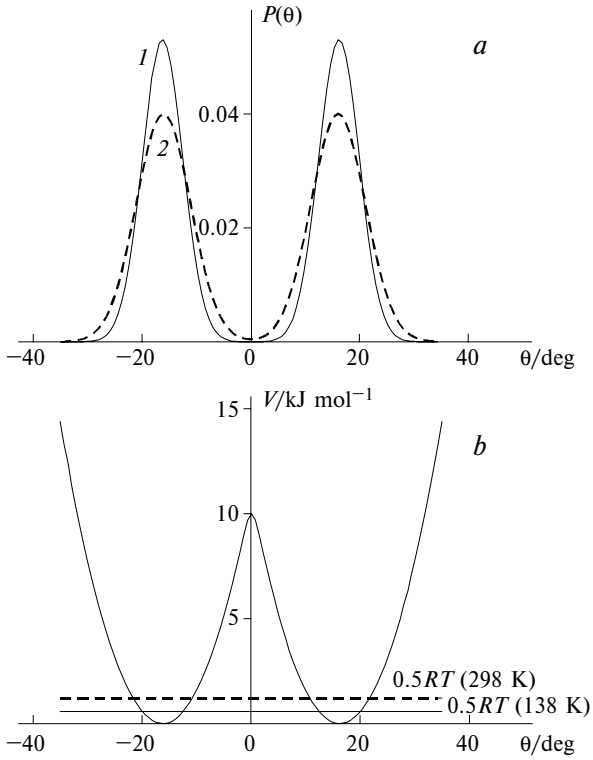

Fig. 5. The probability density functions $P(\theta)$ (*a*) for the librations of the BO_3 fragments about the threefold axis at 138 (*1*) and 298 K (*2*) and the potential-energy curve (*b*) for the librations of the BO_3 fragment in molecule **1** at 138 K.

T_c = 179 K), the central phenyl ring in *para*-terphenyl is disordered over two positions with equal occupancies at temperatures higher than T_c. The orientations of this ring differ in the angle of rotation (by 27°) about the longitudinal axis of the molecule. The calculations[16] demonstrated that this transition is possible due to the low potential barrier between two minima (2.5 kJ mol^{-1}), which is comparable with the value $0.5RT$ (0.8 kJ mol^{-1}) even at 200 K.

In the case under consideration (see Fig. 5), the potential barrier for the BO_3 groups (~10 kJ mol^{-1}) is almost an order of magnitude higher than the energy of thermal vibrations even at room temperature. Evidently, the barrier for the molecule as a whole is still higher. Therefore, the disorder revealed for molecule **1** in the temperature range of 138—298 K is predominantly statistical in nature and the conformational transition between two positions cannot have a substantial effect on QS due to its low probability.

Analysis of the electron density distribution. The applicability of the major concepts of the PQS model to complex **1** is associated with the assumption of the axial symmetry of the electron density distribution about the Fe atom, which is of fundamental importance for establishing the correlation between QS and the geometry of the coordination environment. In the case of octahedral complexes, this assumption was confirmed by both the results of calculations and the experimental data on the electron density distribution. For example, in the deformation electron density map constructed for the quasi-octahedral Fe^{II} complex (sodium nitroprusside), a nearly axial charge distribution about the Fe atom is observed in the equatorial plane (perpendicular to the approximate fourfold axis of the complex).[17]

The presence of the local molecular symmetry C_3 in complex **1** suggests that the electron density distribution is axially symmetrical, which could substantially simplify the analysis of the gradient of the electric field at the ^{57}Fe nucleus as well as of QS caused by this gradient. Taking into account that the previous conclusion about the presence of the axial symmetry in the series of Fe^{II} dioximates has been based exclusively on analysis of

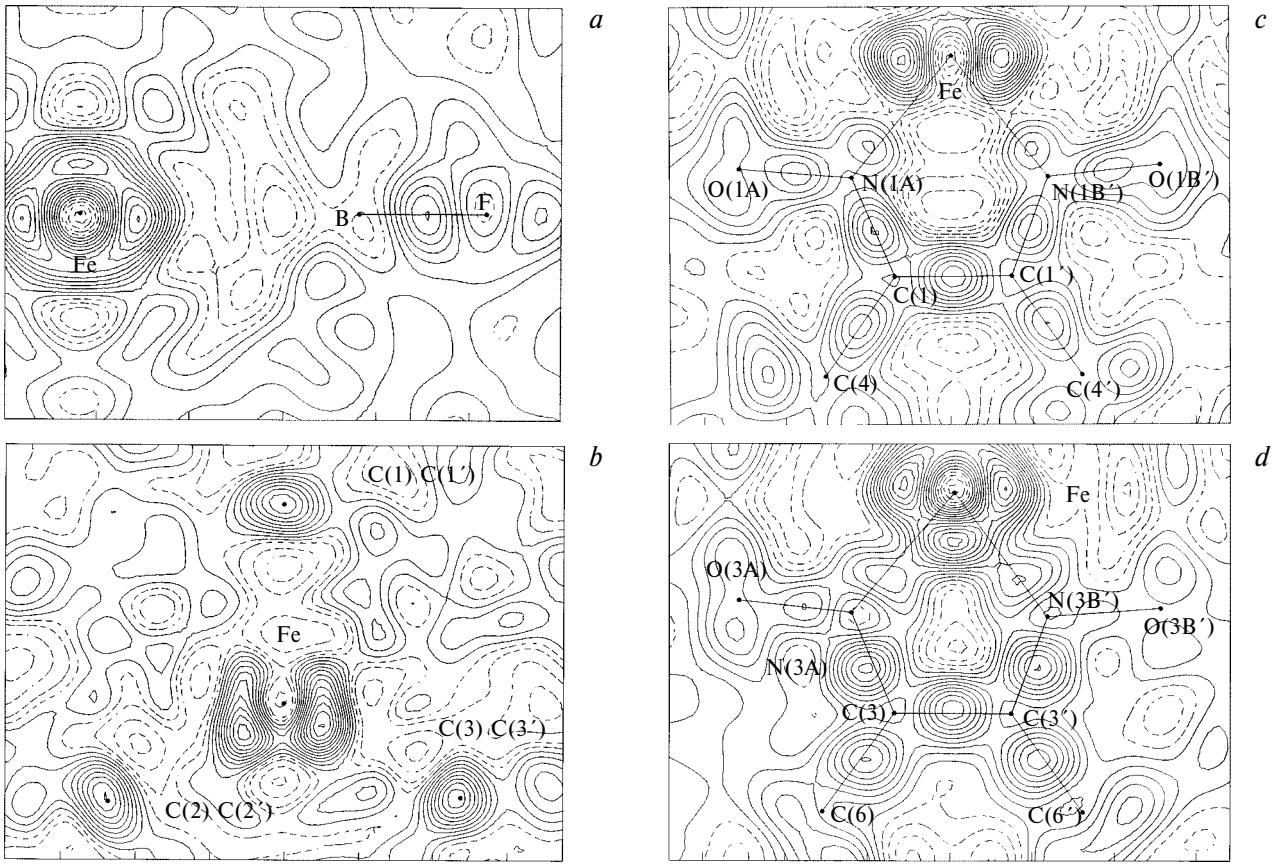

Fig. 6. Sections of the deformation electron density passing through the Fe, B, and F atoms (section *A*) (*a*), through the midpoints of the C(1)—C(1′), C(2)—C(2′), and C(3)—C(3′) bonds (section *B*) (*b*), and in the mean planes of the chelate rings (sections *C* and *D*) (*c* and *d*, respectively). The maps are contoured at intervals of 0.05 e · Å^{-3}; the negative contours are shown as dashed lines. The points in section *A* indicate the positions of the B, F, and Fe atoms; the points in section *B* indicate the positions of the Fe atom and the midpoints of the C(1)—C(1′), C(2)—C(2′), and C(3)—C(3′) bonds; and the points in sections *C* and *D* correspond to the positions of the atoms.

their geometric parameters, we examined the deformation electron density (DED) in the vicinity of the Fe atom calculated based on the X-ray diffraction data.

Examination of the deformation electron density maps for the series of organometallic and inorganic compounds studied previously[18] demonstrated that a substantial anisotropy of the electron density distribution about the metal atoms is observed virtually in all cases. Taking into account that the maxima of the deformation electron density in the vicinity of the metal atom correspond to the partial or complete localization of the molecular orbitals (MO) of the complex at the metal atom, analysis of the positions and relative heights of these maxima makes it possible to perform qualitative analysis of the contribution of the d orbitals to the MOs, which correspond in symmetry to these d orbitals, and to estimate the correctness of the models used for the description of the chemical bonds in organometallic compounds.[19]

The DED maps for molecule **1** were calculated based on the results of the quasi-high-angle refinement of the structure with the use of Dunitz—Seiler' weighting scheme[14] with the parameter $C = 6$ Å^2 using the X-ray diffraction data at 138 K. It was assumed that in this complex (taking into account the trigonal-prismatic symmetry), the d orbitals of the iron(II) atom with the d^6 electronic configuration are split in the strong ligand field into MOs with the symmetry e_1 ($d_{x^2-y^2}$, d_{xy}), a_1 (d_{z^2}), and e_2 (d_{xz}, d_{yz}). In this case, a_1-MO (d_{z^2}) should be nonbonding, doubly degenerate e_1-MO ($d_{x^2-y^2}$, d_{xy}) should be bonding, and doubly degenerate e_2-MO (d_{xz}, d_{yz}) is generally the lowest antibonding MO.[20] Therefore, the metal atom in complex **1**[21] should have the configuration $e_1^4a_1^2e_2^0$ and the electron density would be expected to be accumulated along the threefold axis (a_1-MO (d_{z^2})) and in the equatorial plane passing through the metal atom and the midpoints of the C(1)—C(1′), C(2)—C(2′), and C(3)—C(3′) bonds.

Actually, the maxima of the deformation electron density of height 0.55 e · Å^{-3} were found in the vicinity of the metal atom in the DED sections (Fig. 6) passing through the Fe, B, and F atoms (section *A*) and in the equatorial plane (section *B*). The accumulation of the deformation electron density along the threefold pseudoaxis and in the equatorial plane corresponds to a_1-MO and e_1-MO, respectively. However, unlike the expected axial symmetry of the DED distribution, the corresponding e_1-MO is characterized (see the section *B*) only by the symmetry plane passing through the C(1), C(1′), and Fe atoms (the local symmetry C_s). This plane passes through the molecular threefold axis perpendicular to the crystallographic mirror plane *m*. Therefore, in spite of the equivalence of the geometry of the bidentate ligands, the interaction of the Fe^{II} ion with these ligands (according to the DED maps) is anisotropic. In the above-described sections, accumulation of DED is observed not only in the vicinity of the metal ion but also at the B—F bond in the region corresponding to the lone electron pair of the F atom (section *A*) and at the midpoints of the C—C bonds (section *B*). In turn, an insignificant ellipticity of the latter is indicative of delocalization of the π electrons over the chelate ring.

However, the fact that the displacement of the Fe atom from the center of the prism can lead to the removal of degeneration of e_1-MO and, as a result, to the lowering of the symmetry in the equatorial plane must not be ruled out.

The deformation electron density distributions in the chelate rings of complex **1** are virtually identical. Hence, only two of these distributions will be considered below (see Figs. 6, *c* and *d*). In all sections, the character of accumulation of DED at the C—C, C—Me, C=N, and N—O bonds and in the regions corresponding the lone electron pairs of the N and O atoms is similar. The DED distributions about the Fe^{II} ion (as in the sections shown in Fig. 6) differ substantially. Thus, the accumulation of DED in the vicinity of the central ion is observed in the section *D* (see Fig. 6, *d*) (the sections in the planes of the N(2B′)C(2′)C(2)N(2A) and N(3B′)C(3′)C(3)N(3A) chelate rings are identical). This accumulation corresponds to e_1-MO and is directed toward the C(3)—C(3′) bonds. To the contrary, the local depletion of DED occurs in the corresponding region in the section *C* (see Fig. 6, *c*). At the same time, the accumulation of DED corresponding to a_1-MO is similar in all sections.

Analysis of the experimental data demonstrated that the electron density distribution about the Fe^{II} ion is characterized by the symmetry, which is no higher than C_s. This fact casts doubt on the applicability of the PQS model to the analysis of QS in complex **1**. It should be noted that the distortion of the electron density distribution about the metal ion introduced by the disorder should be small due to the statistical nature of the latter and this distortion has virtually no effect on the metal atom. Apparently, the disorder does not affect the qualitative pattern of the electron density distribution in complex **1**.

The results obtained in the present work did not confirm the occurrence of the structural phase transition in the crystal of **1**, which has been assumed previously. The observed difference between the experimental QS values and those calculated within the framework of the PQS model results from the fact that two major concepts of the PQS model are not true for complex **1**: (1) the Fe^{II} ion is displaced from the center of the coordination polyhedron along the threefold axis of the molecule resulting in the nonequivalence of the contributions of the N atoms to the QS values and (2) the axial symmetry of the electron density distribution about the central atom is distorted.

The anisotropy of the electron density observed in the $FeDm_3(BF)_2$ complex may be caused both by the displacement of the Fe^{II} ion from the center of the coordination polyhedron and the effect of the molecular packing. However, the fact that this distribution is a characteristic feature of this type of clathrochelate com-

plexes could not be excluded. Hence, it is of interest to compare our results with the results of precision studies of "classical" representatives of this series, in the crystal structures of which the iron ion is not displaced and the disorder of the clathrochelate core is absent.

We thank V. E. Zavodnik for helpful discussion.

This work was financially supported by the Russian Foundation for Basic Research (Project Nos. 00-03-32-807a, 00-15-97359, and 99-03-3298a).

References

1. Ya. Z. Voloshin, *Ros. Khim. Zh.* (*Zh. Ros. Khim. Obshch. im. D. I. Mendeleeva)*, 1998, **42**, 5 [*Mendeleev Chem. J.*, 1998, **42** (Engl. Transl.)].
2. I. I. Vorontsov, K. A. Potekhin, M. Yu. Antipin, and Ya. Z. Voloshin, *School-Conference for Young Scientists "Organometallic Chemistry Towards the 21st Century," Oral Presentations and Posters,* Moscow, 1999, 60.
3. Ya. Z. Voloshin, N. A. Kostromina, and A. Yu. Nazarenko, *Inorg. Chim. Acta*, 1990, **170**, 181.
4. Ya. Z. Voloshin, N. A. Kostromina, A. Yu. Nazarenko, and E. V. Polshin, *Inorg. Chim. Acta*, 1991, **185**, 83.
5. Ya. Z. Voloshin, T. E. Kron, V. K. Belsky, V. E. Zavodnik, Y. A. Maletin, and S. G. Kozachkov, *J. Organomet. Chem.*, 1997, **537**, 207.
6. S. Lindeman, Yu. T. Struchkov, and Ya. Z. Voloshin, *J. Coord. Chem.*, 1993, **28**, 319.
7. G. M. Bankroft, *Coord. Chem. Rev.*, 1973, **11**, 247.
8. A. Y. Nazarenko, E. V. Polshin, and Ya. Z. Voloshin, *Mendeleev Commun.*, 1993, 45.
9. S. C. Jackels and N. J. Rose, *Inorg. Chem.*, 1973, **12**, 1232.
10. V. A. Strel´tsov and V. E. Zavodnik, *Kristallografiya*, 1989, **34**, 1369 [*Sov. Phys. Crystallogr.*, 1989, **34** (Engl. Transl.)].
11. G. M. Sheldrick, *SHELXTL-PLUS, Release 5.0*, Siemens Analytical Instruments Inc., Madison, Wisconsin, USA, 1994.
12. I. E. Zanin, M. Yu. Antipin, and Yu. T. Struchkov, in *Problemy kristallokhimii* [*Problems of Crystal Chemistry*], Nauka, Moscow, 1991, 65 (in Russian).
13. V. Schomaker and K. N. Trueblood, *Acta Crystallogr.*, 1968, **24B**, 63.
14. J. D. Dunitz and P. Seiler, *Acta Crystallogr.*, 1973, **29B**, 589.
15. T. Maverick and K. N. Trueblood, *THMA-11, Thermal Motion Analysis Program*, Zurich, 1987.
16. J. L. Baudour, H. Cailleau, and W. B. Yelon, *Acta Crystallogr.*, 1977, **33B**, 1773.
17. M. Yu. Antipin, V. G. Tsirel´son, M. P. Flyugge, Yu. T. Struchkov, and R. P. Ozerov, *Koord. Khim.,* 1987, **13**, 121 [*Sov. J. Coord. Chem.,* 1987, **13** (Engl. Transl.)].
18. A. A. Low and M. B. Hall, in *Theoretical Models of Chemical Binding, Part 2, The Concept of the Chemical Bond*, Ed. Z. B. Maksiz, Springer-Verlag, Berlin, 1990, 543.
19. M. Yu. Antipin, K. A. Lysenko, and R. Boese, *J. Organomet. Chem.*, 1996, **508**, 259.
20. E. Larsen, G. N. La Mar, B. E. Wagner, J. E. Parks, and R. H. Holm, *Inorg. Chem.*, 1972, **11**, 2652.
21. W. M. Reiff, *J. Am. Chem. Soc.*, 1973, **95**, 3048.

Received May 10, 2000